Hindawi
Geofluids
Volume 2019, Article ID 5602648, 11 pages
https://doi.org/10.1155/2019/5602648

Research Article

Geochemical Modeling of Water-Rock Interaction in the Granulite Rocks of Lower Crust in the Serre Massif (Southern Calabria, Italy)

Carmine Apollaro

University of Calabria, Department of Biology, Ecology and Earth Sciences (DIBEST), 87036 Rende, Italy

Correspondence should be addressed to Carmine Apollaro; apollaro@unical.it

Received 10 November 2018; Accepted 1 January 2019; Published 14 March 2019

Guest Editor: Giovanni Mongelli

To simulate the evolution of groundwaters interacting with granulitic rocks of the lower crust exposed in the southern sector of the Calabrian region, reaction path modeling was performed by means of the EQ3/6 software package version 8.0a. Low-salinity waters issuing from granulite have Na–Cl to Na-HCO_3 composition, about neutral pH (mean value of 6.7), outlet temperatures of 7.7 to 14.2°C, oxidant redox potentials from 100 to 182 mV, and electrical conductivity from 72.1 to 196.9 μS/cm. The mineral constituents of local granulite are plagioclase, amphibole, biotite, clinopyroxene, garnet, and orthopyroxene. Simulations were carried at constant temperature of 11.8°C (which reproduces the average temperature of local groundwaters) fixing the fugacity of CO_2 at $10^{-2.4}$ bar (mean value), $10^{-2.0}$ bar (mean value +1 σ), and $10^{-2.8}$ bar (mean value -1 σ). The analytical contents of major elements in groundwaters were satisfactorily reproduced by modeling and are fully consistent with the secondary minerals produced by weathering processes affecting the same rocks.

1. Introduction

The chemical composition of natural water is derived from many different sources of solutes, including aerosols and gases from the atmosphere, erosion and weathering of soil and rocks, and dissolution or precipitation reactions occurring below the land surface. However, human activities play an important and not negligible role on the chemical composition of natural waters. Some of the processes of dissolution or precipitation of minerals can be closely evaluated by means of principles of chemical equilibrium whereas other processes are irreversible and require consideration of reaction mechanisms and rates [1–4]. During water rock-interaction, the major, minor, and trace constituents are leached from primary minerals and enriched into local groundwaters. At the same time, during the progressive dissolution of the rocks, the aqueous solution may attain saturation with respect to different secondary solid phases, potentially acting as sinks of various elements and species [5–9]. For these reasons, the fate of the chemical components of interest during weathering of rocks is a rather complex theme, whose understanding requires the use of reaction path modeling [10–20]. In this work, the EQ3/6 software package, version 8.0a [21], was used to study the weathering processes that occurred on the granulite rocks of the Serra Massif. Reaction path modeling was performed using some needful information, comprising (i) relevant thermodynamic and kinetic data, (ii) chemical composition and abundance of each primary solid phase of interest, (iii) chemical composition of the initial aqueous solution, and (iv) chemical composition of the aqueous solution during water–rock interaction. Items (i) to (iii) are needed to implement reaction path modeling, whereas item (iv) is used to evaluate its validity, through comparison of computed results with analytical data.

2. Geological Background

The Calabrian belt, known as the Calabrian-Peloritan Arc [22], belongs to a fold belt linking the NW-SE Apennines

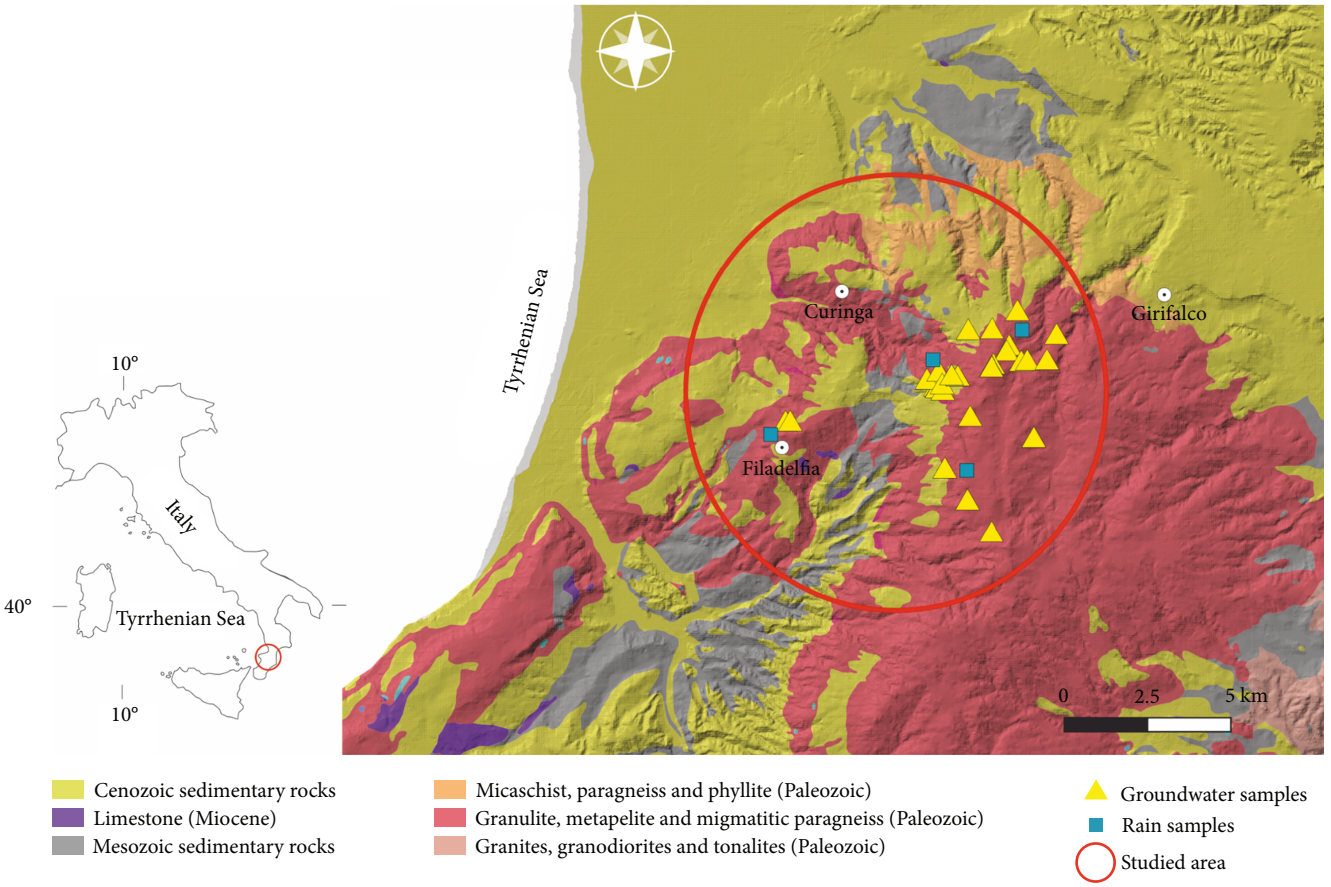

FIGURE 1: Simplified geological map of the study area also showing the location of spring water and rainwater samples.

structure with W-E-trending structures of Sicily and Northern African Maghrebian regions [23].

On the basis of radiometric, petrological, and seismic data [24], the Calabrian Peloritan Arc (CPA) has been considered to have a pre-Hercynian lower crustal segment thrust into the middle crust during the Hercynian orogeny and uplifted during the Europe-Apulia collision in Oligocene-Early Miocene ([22, 25] and references therein).

CPA is divided into two main sectors: (i) the northern sector, in which fall the Sila Massif and Coastal Chain, and (ii) southern sector, in which fall Aspromonte and Serre Massifs. The two sectors are separated by a strike-slip tectonic line cross along the Catanzaro trough [26]. The study areas fall in the Serre Massif which is made up mainly of high- and low-grade metamorphic rocks that discontinuously overlay the late Hercynian granitoids, granodiorites, and tonalites. All the sequences are sometimes covered by unmetamorphosed Cenozoic sedimentary deposits [27]. In the studied area (Figure 1), granulite-facies crop up extensively. These rocks can be associated with two distinct tectonic units belonging to the Monte Gariglione and Polia-Copanello complexes of the Sila Unit ([22, 28]; Bonardi et al., 2001). The two lithostratigraphic units [29] consist in (i) the lower unit mainly made up of metabasic rocks, predominantly layered metagabbro, and meta-anorthosite with small and subordinate ultramafic bodies and in (ii) the upper unit made up of migmatitic aluminous paragneiss, orthopyroxene-bearing felsic granulite, and marbles that sometimes include quartz monzo-gabbronorite sills and/or dikes. Surrounding the investigated area, the granulite-facies rocks and phyllonitic rocks are separated by the Curinga-Girifalco Line of Alpine age [29].

3. Methods

3.1. Water Sampling and Analytical Techniques. A total of 30 spring water samples and 4 local rainwaters were collected in the study area (Figure 1) and analyzed for major components. During the collection samples, unstable parameters, such as temperature, pH, and oxidation-reduction potential (Eh) as well as electrical conductivity (EC), were measured in the field by using portable instruments. Total alkalinity was also determined in the field by acidimetric titration utilizing HCl 0.01 N as titrating agent. Waters were filtered in situ through a 0.4 μm pore-size polycarbonate membrane filter (Nuclepore). Samples for the determination of anions were stored without further treatment. Samples for the determination of cations were acidified, by addition of suprapure acid (1% HNO_3) after filtration and stored. New polyethylene bottles were used for all the samples. In the laboratory, the concentrations of Na^+, K^+, Mg^{2+}, Ca^{2+}, F^-, Cl^-, SO_4^{2-}, and NO_3^- were determined by high-performance liquid chromatography (HPLC, Dionex DX 1100). All the chemical data were determined in the laboratory of the Department of

Table 1: Chemical-physical parameters of groundwater samples coming from the study.

Code	Temp °C	pH	Eh (mV)	Cond (μs/cm)	Na (mg/L)	K (mg/L)	Ca (mg/L)	Mg (mg/L)	Alk Tot (mg/L)	SO_4 (mg/L)	Cl (mg/L)	NO_3 (mg/L)	SiO_2 (mg/L)	F (mg/L)
1	13.30	6.8	123.0	193.9	14.6	1.9	11.2	4.7	60.5	8.1	20.0	16.5	20.3	0.1
2	12.80	6.0	120.0	92.8	8.3	1.1	2.5	1.4	12.8	6.8	11.8	1.2	10.8	0.1
3	12.50	6.7	100.0	118.5	10.4	0.9	4.0	2.9	23.6	5.3	16.1		19.3	0.1
4	12.40	6.7	102.0	100.7	8.5	0.9	3.1	2.8	15.1	6.2	13.0		15.0	0.1
5	12.10	6.5	107.0	103.6	10.0	1.1	3.6	1.9	22.8	4.3	15.1		14.8	0.1
6	12.10	6.0	128.0	105.9	9.3	1.1	4.0	2.1	18.1	12.1	12.4	1.1	11.8	0.0
7	11.80	6.7	107.0	147.4	11.2	1.2	6.0	2.7	19.9	8.5	19.7	0.6	15.8	0.1
8	12.20	6.8	121.0	125.0	12.0	1.0	5.0	2.2	37.2	3.6	12.9		25.3	0.1
9	12.60	6.2	133.0	106.1	9.3	1.1	3.6	2.0	20.5	4.3	15.1	4.1	24.5	0.1
10	12.40	6.3	117.0	92.6	8.5	0.9	2.6	1.6	11.9	7.4	13.3	0.7	13.8	0.1
11	12.30	6.3	121.0	123.2	9.8	1.1	5.4	3.6	33.5	5.0	14.5	3.3	17.0	0.1
12	12.50	6.8	110.0	133.8	9.6	0.8	6.6	3.5	39.7	3.0	9.2	2.4	22.3	0.1
13	11.40	7.2	103.0	140.3	10.9	1.1	7.9	3.1	38.9	6.0	13.6	1.1	28.5	0.1
14	11.40	6.3	131.0	109.3	10.7	1.1	3.1	1.5	13.8	4.3	18.5	1.9	18.5	0.1
15	11.30	6.3	138.0	72.1	7.1	0.4	1.8	0.8	7.4	4.0	11.0	0.2	13.5	0.0
16	11.20	6.5	129.0	86.5	8.2	0.6	2.4	1.0	11.3	4.3	12.0	0.7	15.8	0.0
17	10.90	6.9	118.0	126.8	10.9	1.0	5.3	2.0	27.9	3.1	14.9	0.4	37.5	0.1
18	11.90	7.1	110.0	112.1	9.0	0.8	4.2	2.5	26.7	5.9	11.9	2.2	53.5	0.1
19	10.30	7.2	108.0	110.4	8.9	0.9	4.8	2.3	21.1	4.0	14.9	0.0	41.8	0.1
20	9.60	6.4	138.0	92.1	8.1	1.0	2.5	1.7	17.3	3.4	12.7	1.0	26.5	0.1
21	11.50	8.2	111.0	177.6	9.0	2.2	9.5	7.1	41.7	17.4	11.2		35.3	0.1
22	9.60	7.3	100.0	101.4	9.7	0.8	4.1	2.2	21.6	5.0	13.3	3.9	23.8	0.1
23	12.40	6.3	105.0	92.8	7.7	0.9	4.6	1.9	27.5	5.0	9.1	0.9	22.5	0.1
24	7.70	6.8	135.0	116.5	9.0	0.9	6.2	2.4	32.2	4.5	13.2	3.0	31.3	0.1
25	10.40	6.2	140.0	86.6	7.4	0.7	2.9	1.3	14.5	4.4	11.3	0.5	11.3	0.0
26	11.70	7.1	100.0	127.1	9.6	0.9	5.4	2.9	35.4	3.1	8.1	1.3	13.2	0.1
27	11.80	7.1	102.0	196.9	13.5	1.5	8.6	5.0	35.7	3.4	28.5	0.6	16.5	0.1
28	13.30	6.4	168.0	108.2	8.6	0.9	2.6	1.5	15.8	4.1	12.8		11.6	0.1
29	13.10	6.3	182.0	97.3	8.1	0.7	2.5	1.4	15.9	4.8	10.8		11.3	0.1
30	14.20	6.6	158.0	115.3	9.5	0.9	3.0	2.0	21.0	3.8	14.3		14.7	0.1

Table 2: Chemical-physical parameters of rainwater samples coming from the study area.

	pH	Ca (mg/L)	Mg (mg/L)	Na (mg/L)	K (mg/L)	HCO_3 (mg/L)	SO_4 (mg/L)	Cl (mg/L)	SiO_2 (mg/L)
Rain 1	5.62	2.60	0.60	6.80	0.31	7.42	3.65	10.49	9.65
Rain 2	6.50	1.30	0.33	6.20	0.94	10.1	4.56	9.40	9.33
Rain 3	6.20	2.30	0.35	12.40	1.40	5.62	3.26	13.20	5.64
Rain 4	6.33	0.90	0.30	8.60	0.60	6.98	4.23	12.41	7.10

Biology, Ecology and Earth Sciences of the University of Calabria, and are reported in Tables 1 and 2.

3.2. Chemical Characterization of Rocks and Minerals. The mineralogical and chemical characteristics of the granulite considered as a dissolving reactant in this work is based on the study of Apollaro et al. [30] who collected and analyzed several granulite samples from the lower crust exposed in the southern sector of the Calabrian region.

Apollaro et al. [30] carried out modal analyses on granulite-bearing plagioclase rock lithotypes (e.g., [31, 32]) to determine the volume percentages of main and accessory minerals by optical microscopy of thin sections using a mechanical stage. Granulite rocks have a coarse-grained

texture and are plagioclase-rich (60%) with minor amounts of amphibole (10%), biotite (10%), clinopyroxene (8%), garnet (8%), and orthopyroxene (4%).

3.3. Geochemical Modeling. Reaction path modeling of progressive dissolution of granulite in rainwater was carried out by means of the software package EQ3/6, version 8.0a [21], utilizing the thermodynamic database of Wolery and Jove-Colon [33]. Three simulations were performed in kinetic (time) mode, under a closed system with secondary solid phases and an open system with CO_2, adopting different, constant P_{CO2} values ($10^{-2.0}$, $10^{-2.4}$, and $10^{-2.8}$ bar) and at constant temperature of 11.8°C (which reproduces the average temperature of local groundwaters).

Based on the mineralogical and petrographic data, the dissolving granulite was considered to be constituted by plagioclase, amphibole, biotite, clinopyroxene, garnet, and orthopyroxene. Kinetic parameters and surface area were specified for each primary (dissolving) solid phase because reaction path modeling was performed in time mode (Table 3). Kinetic parameters were obtained from the compilation and critical review of available laboratory dissolution experiments [34]. Thermodynamic data of some minerals such as anorthite, K-feldspar, albite, annite, phlogopite, muscovite, 1.4 nm clinochlore, magnesite, calcite, rhodochrosite, siderite, witherite, strontianite, and aragonite were evaluated by a review work of Helgeson et al. [35]. Thermodynamic data of clay minerals (Mg, Na, K, and Ca end members of beidellite, saponite, and montmorillonite) and 1.4 nm chamosite and celadonites were calculated by Wolery and Jove-Colon [33] and references therein. Those of vermiculites such as Me-Al vermiculites, Me-Fe vermiculites, Me-Mg-Al vermiculites, and Me-Mg-Fe vermiculites with Me=Na, K, Mg, and Ca were evaluated by Apollaro et al. [36, 37]. From Perri et al. [38], thermodynamic data of illite were obtained, and those of ferrihydrites are from the work of Majzlan et al. [39].

Four chemical analyses of rainwaters collected in the study area (Table 2) were used to compute the chemical composition of the initial aqueous solution (mean value).

4. Water Chemistry

4.1. Water Classification. Low-salinity waters issuing from granulite have about neutral pH (mean value of 6.7), outlet temperatures of 7.7° to 14.2°C, oxidant redox potentials from 100 to 182 mV, and electrical conductivity from 72.1 to 196.9 μS/cm. Based on the triangular plots of major anions and major cations (Figure 2), the waters show a Na-Cl to Na-HCO_3 composition.

In the binary diagram of pH vs. P_{CO2} (Figure 3(a)), most of the waters are within the soil range (0.002–0.04 bar; [40]); only 2 samples are positioned below the lower soil threshold.

Therefore, in the area, CO_2 is prevailingly contributed by biogenic shallow sources, such as the decay of organic matter and root respiration occurring in the rhizosphere. The plot of the calcite saturation index vs. pH (Figure 3(b)) shows that undersaturation with calcite is a common condition for all waters.

Table 3: Geometrical surface areas and masses of solid phases of interest.

Mineral	Vol %	Initial surface area (cm^2)	Vm (cm^3/mol)	Mass (mole)
Plagioclase	60	84000	100.11	13.98462
Amphibole	10	14000	139.2	1.67625
CPX	8	11200	100.25	1.86201
OPX	4	5600	138.665	0.67309
Garnet	8	11200	272.92	0.68396
Biotite	10	14000	152.27	1.53237

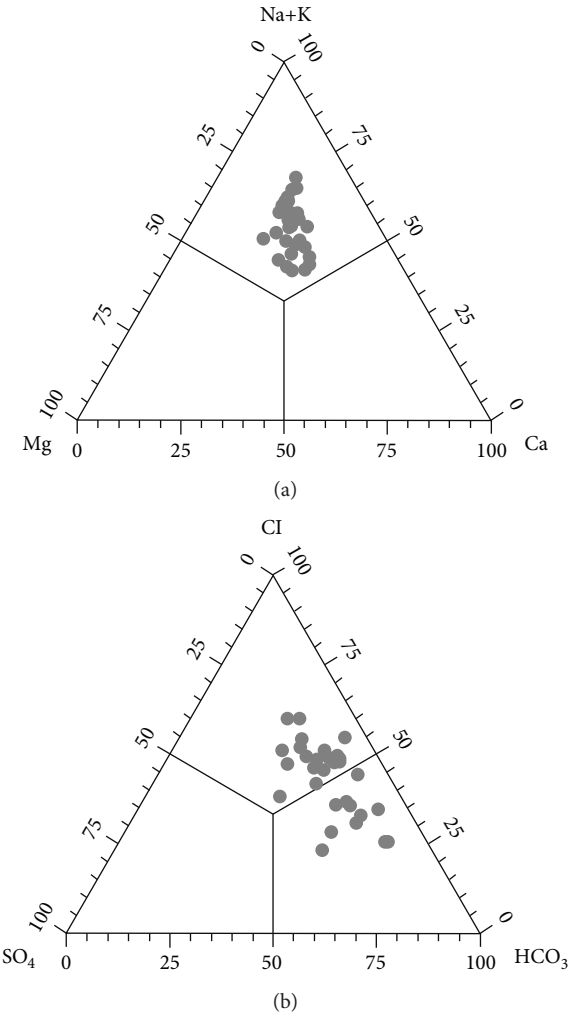

Figure 2: Triangular plots of major anions and major cations for the 30 groundwater samples from the study area.

5. Interpretation of Reaction Path Modeling

Analytical data of the groundwaters from the granulitic aquifer of the lower crust exposed in the southern sector of the Calabrian region were compared with results of reaction path modeling. For the waters of interest, alkalinity is used as a reaction progress variable (Xi) instead of pH for the following reasons [13]: (i) the progressive

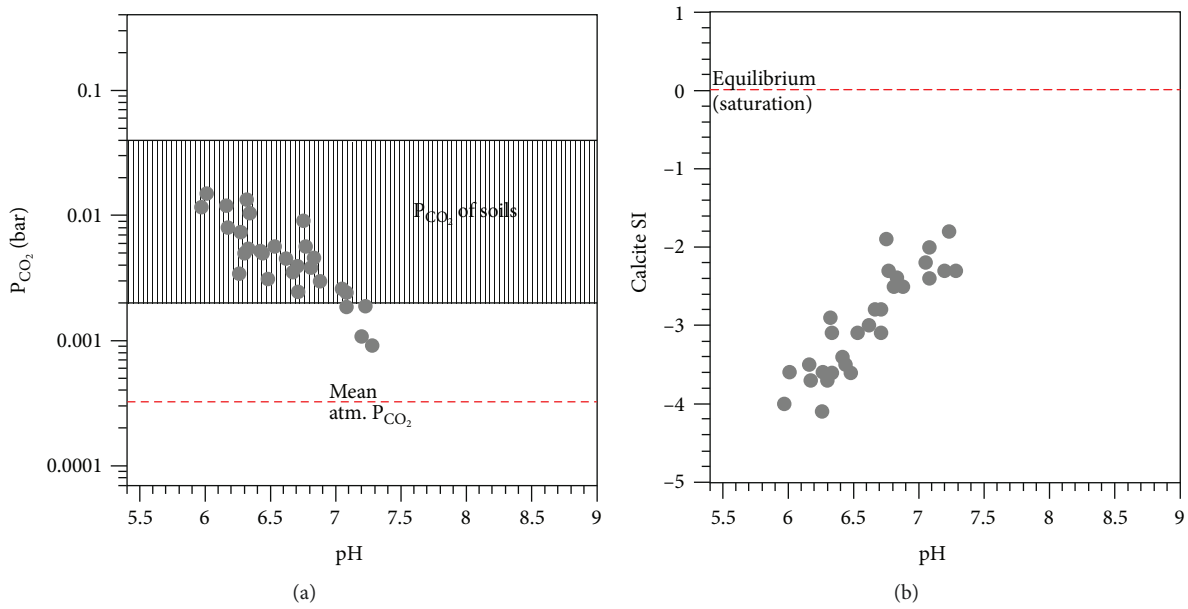

FIGURE 3: (a) Correlation diagram of pH vs. P_{CO2} also showing the range of soil P_{CO2} [40] and the mean atmospheric P_{CO2} value. (b) Correlation diagram of pH vs. calcite saturation index.

dissolution of primary solid phases, driven by conversion of aqueous CO_2 to HCO_3^- ion, causes a continuous increase in alkalinity, (ii) precipitation of calcite, which would cause a decrease in alkalinity, is limited (see Section 4.1), and (iii) the alkalinity consumption due to acidity produced by oxidative dissolution of pyrite is negligible, as indicated by the generally low SO4 concentrations.

Indeed, during water-rock interaction, due to the appearance of different secondary mineral assemblages acting as pH buffers (e.g., [41–44]), pH changes are quite irregular and less continuous.

Figure 4 shows a close-to-linear relation between Xi and alkalinity, with a good correspondence for all different pCO_2 values considered.

The simulations show a progressive dissolution dominated by plagioclase followed by a minor amount of amphibole, clinopyroxene, and biotite and negligible amounts of orthopyroxene and garnet for all the investigated pCO_2 (Figure 5).

As already shown by Apollaro et al. [30], the differences in the type and amount, along the reaction path of the secondary minerals (Figure 6), mainly reflect the different dissolutions of primary minerals and, therefore, a different contribution during the reaction, of chemical elements.

The two main secondary solid phases forming during granulite dissolution, appearing at alkalinity close to 5 mg HCO_3/L, are kaolinite and vermiculites with minor amount of hydroxides. Kaolinite, vermiculites, and hydroxides act as sinks of Al, Si, and Fe released by primary dissolved minerals. Carbon dioxide partial pressure has a significant influence on the first appearance of product phases for all these minerals except kaolinite. The lower the pCO_2, the earlier all the secondary phases begin to precipitate.

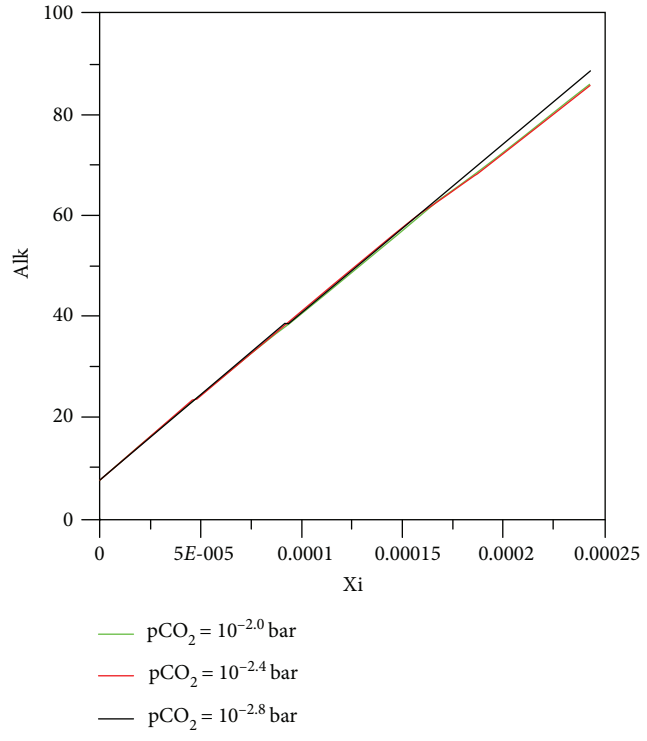

FIGURE 4: Plot of alkalinity vs. the reaction progress variable showing the results of reaction path modeling for the dissolution of granulite under different fCO_2 values (see legend).

Consistently with the undersaturation with calcite, there is no solid carbonate.

5.1. The Aqueous Solution. The theoretical path of granulite dissolution, at constant pCO_2 of $10^{-2.0}$, $10^{-2.4}$, and $10^{-2.8}$ bar,

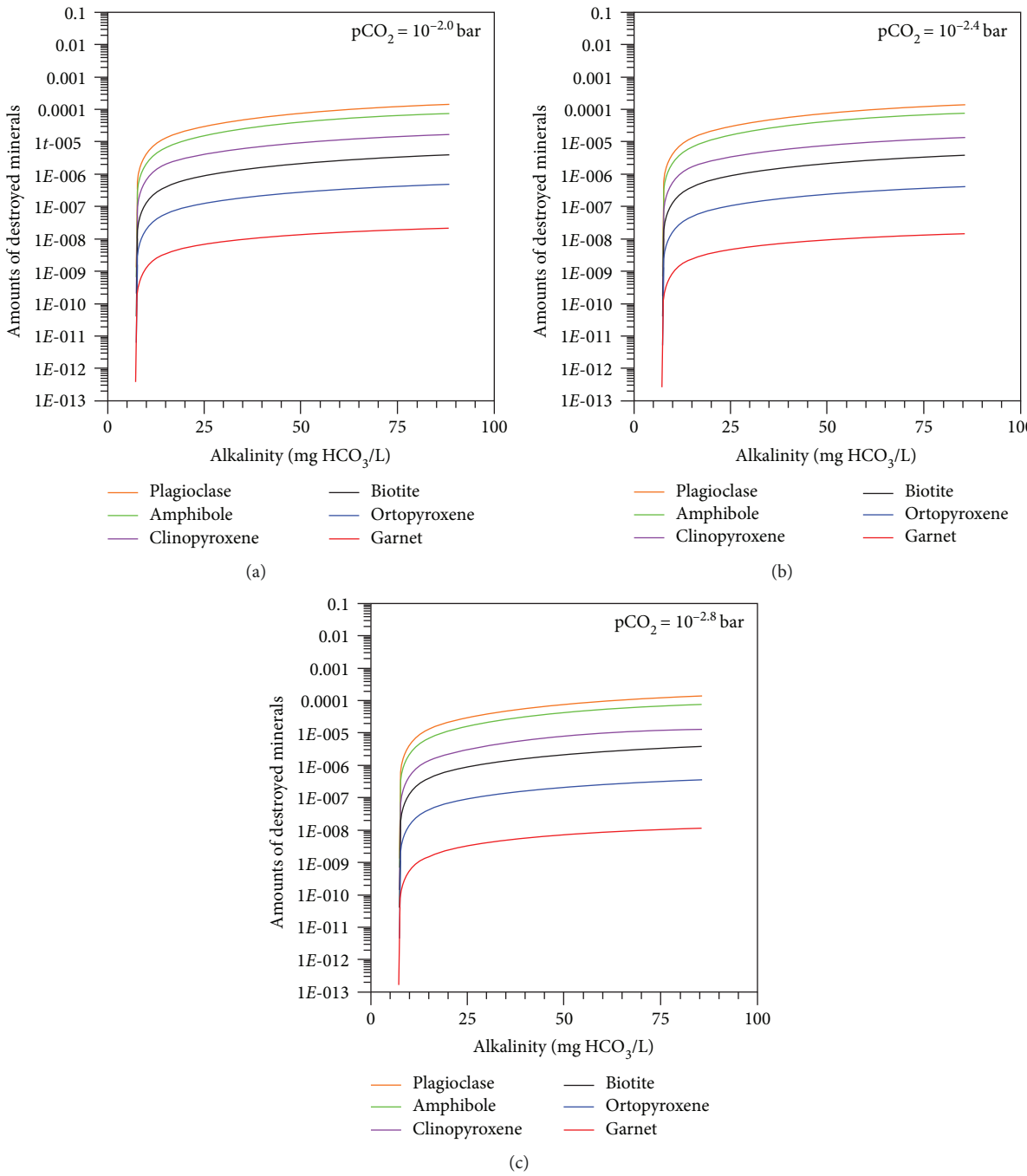

Figure 5: Moles of destroyed solid reactants against alkalinity, showing the results of reaction path modeling for the dissolution of granulite: (a) pCO_2 of $10^{-2.0}$ bar, (b) pCO_2 of $10^{-2.4}$ bar, and (c) pCO_2 of $10^{-2.8}$ bar.

indicates that the water-rock interaction is dominated by dissolution of plagioclase, amphibole, and clinopyroxene and much less from biotite, orthopyroxene, and garnet (Figure 5). The concentration of aqueous Ca and Mg (Figure 7) increases owing to dissolution of plagioclase, amphibole, and clinopyroxene, and the amount of Ca and Mg incorporated in precipitating secondary minerals is negligible. Variable pCO_2 does not affect the Ca/HCO_3 and Mg/HCO_3 ratio at the three pCO_2 values, and there is a very good agreement between reaction path modeling results and the analytical data (Figure 7).

The binary plots of Na versus alkalinity and K versus alkalinity (Figure 8) highlight that the dissolved Na and K concentrations increase slightly through the whole simulation, since the amounts of Na and K contributed by dissolution of plagioclase and biotite are minimal, and a part of K and Na is incorporated in the vermiculites at all pCO_2 (Figure 6). As already shown by Apollaro

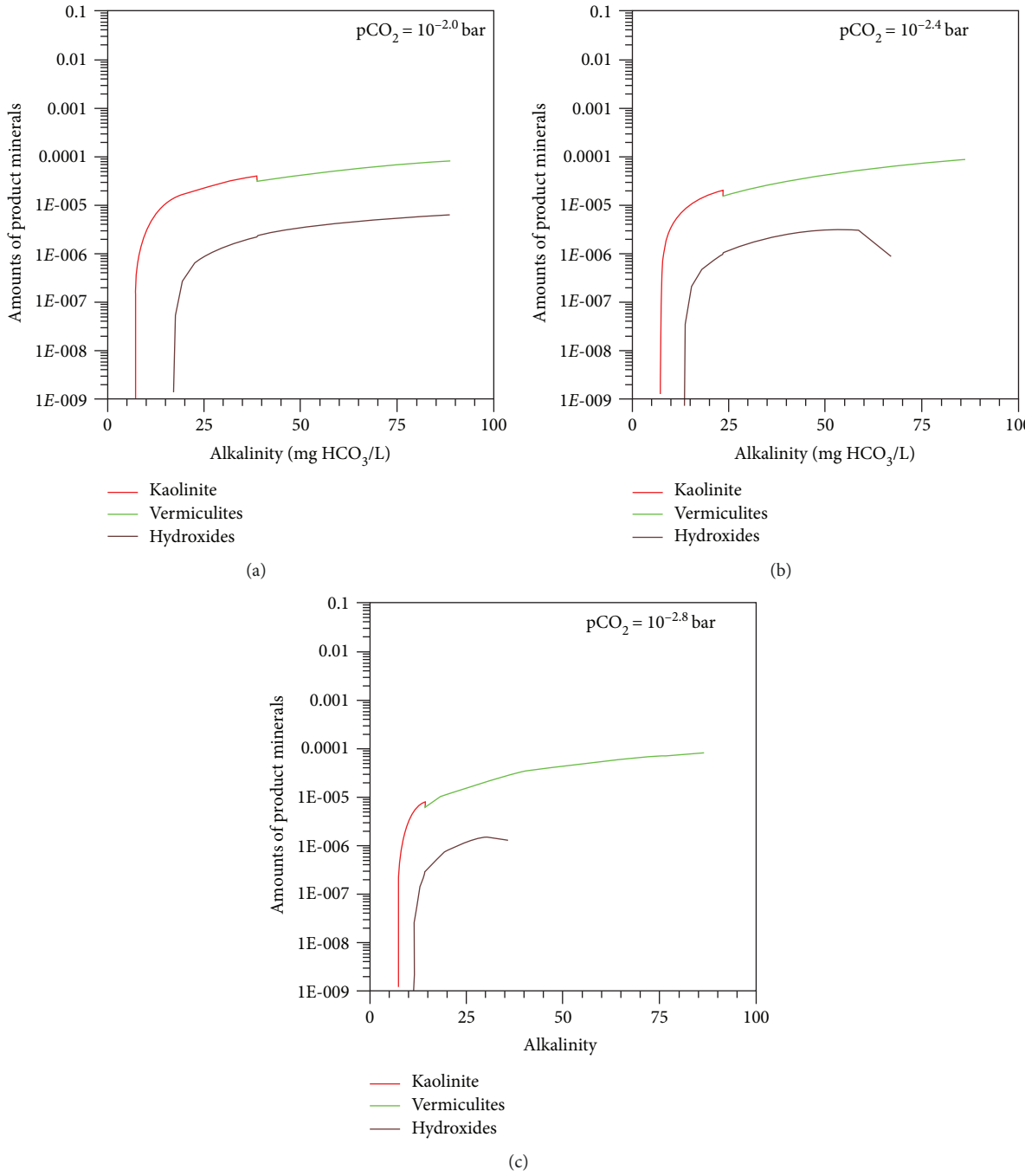

Figure 6: Moles of solid product phases against alkalinity, showing the results of reaction path modeling for the dissolution of granulite (a) pCO_2 of $10^{-2.0}$ bar, (b) pCO_2 of $10^{-2.4}$ bar, (c) pCO_2 of $10^{-2.8}$ bar.

et al.,[13] Na and K versus alkalinity plots in low TDS groundwaters are poorly informative because these two alkali metals are probably controlled by varying contributions of atmospheric-marine salts rather than the water-rock interaction.

The binary plots of SiO_2 versus alkalinity (Figure 9) highlight that the concentration of aqueous SiO_2 increases during the dissolution of granulite because all minerals present in the rocks contain SiO_2 and the amount of SiO_2 incorporated in precipitating kaolinite and vermiculite is subordinate. Similar to Ca and Mg, variable pCO_2 does not affect the SiO_2/HCO_3 ratio and there is a very good agreement between analytical data and results of reaction path modeling.

6. Conclusion

Geochemical prospecting carried out in the granulitic rocks exposed in the southern sector of the Calabrian region (Southern Italy) has allowed identification of several springs

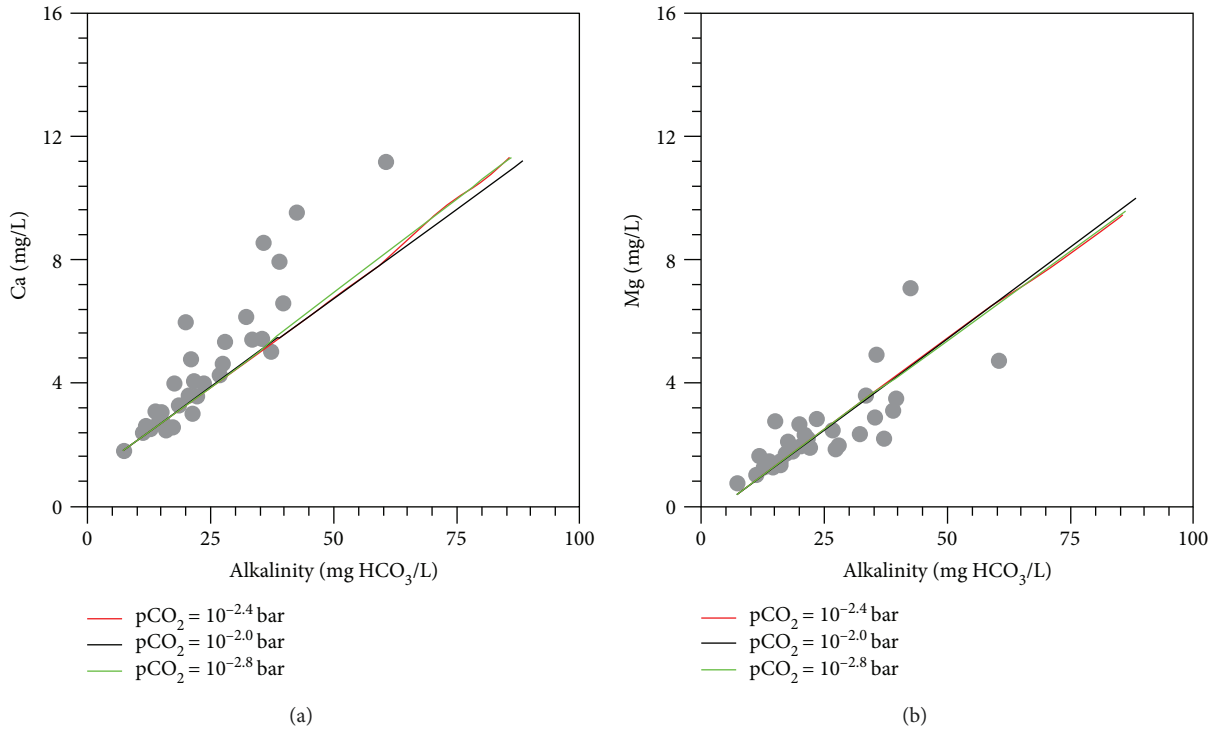

FIGURE 7: Plots of (a) Ca and (b) Mg vs. alkalinity showing the analytical data from groundwaters interacting with granulitic rocks of the lower crust as well as the results of reaction path modeling for granulite dissolution under different pCO_2 (see legend).

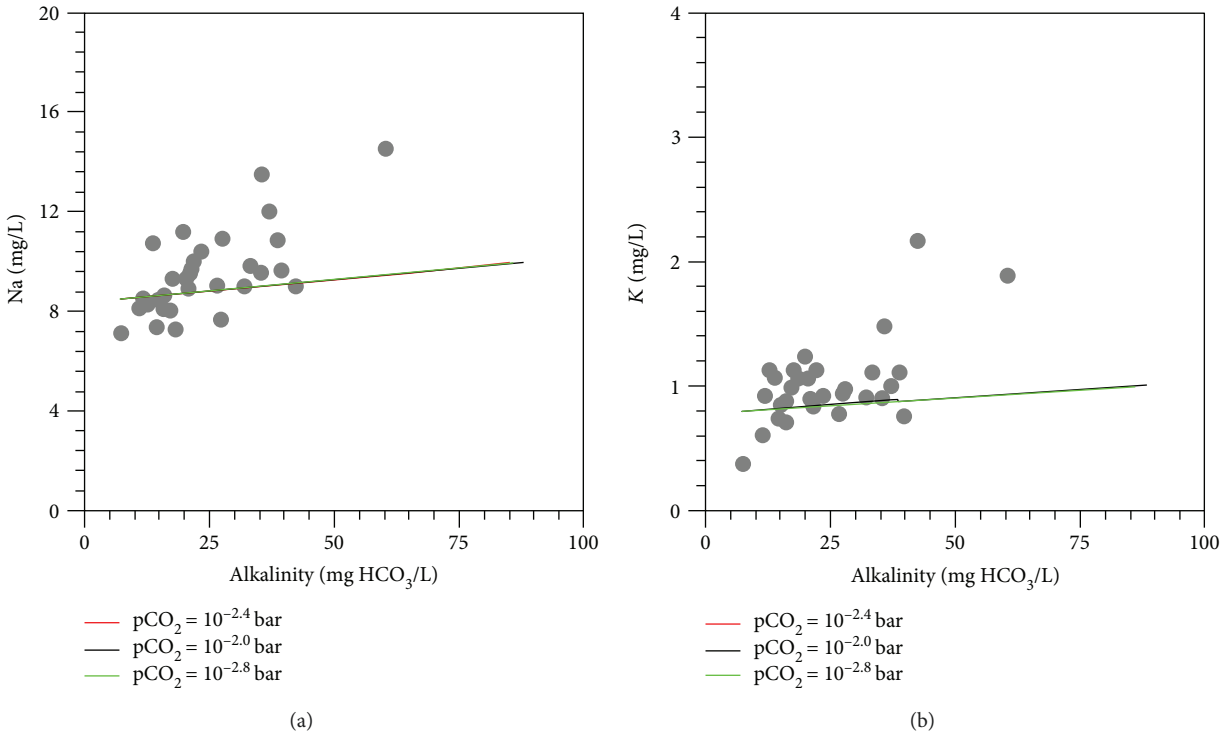

FIGURE 8: Plots of (a) Na and (b) K vs. alkalinity showing the analytical data from groundwaters interacting with granulitic rocks of the lower crust as well as the results of reaction path modeling for granulite dissolution under different pCO_2 (see legend).

hosted in a very extensive shallow hydrogeological metamorphic complex. To evaluate the irreversible water-rock mass exchanges occurring during the evolution of rainwaters to groundwaters, a reaction path modeling in kinetic (time) mode was performed, under a closed system with secondary solid phases and an open system with CO_2, adopting

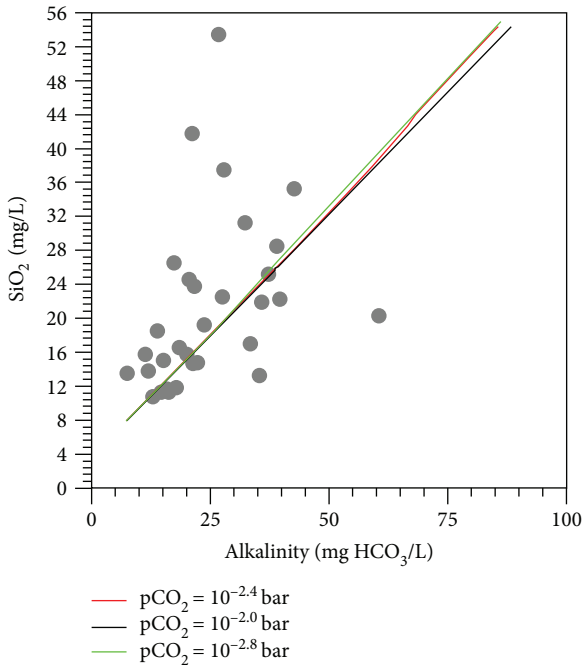

FIGURE 9: Plots of SiO_2 vs. alkalinity showing the analytical data from groundwaters interacting with granulitic rocks of the lower crust as well as the results of reaction path modeling for granulite dissolution under different pCO_2 (see legend).

different, constant pCO_2 values ($10^{-2.0}$, $10^{-2.4}$, and $10^{-2.8}$ bar) and at constant temperature of 11.8°C.

The secondary (product) solid phases that were allowed to precipitate are kaolinite, vermiculite solid mixture, and hydroxide solid mixture according to the general understanding of chemical weathering and the results obtained by Apollaro et al. [30] who studied the weathering processes affecting the same rocks.

The results of reaction path modeling show that the release of major dissolved constituents to shallow groundwaters is mainly controlled by weathering of plagioclase accompanied by minor amounts of amphibole, clinopyroxene, and biotite and negligible amounts of orthopyroxene and garnet. Computed contents of key dissolved components (Ca, Mg, Na, K, and SiO_2) are comparable with analytical data, although not all the details are reproduced, probably due to insertion in the model of the average composition of primary minerals, in spite of their nonnegligible chemical variations and to the fact that some elements such as Na and K are controlled by varying contributions of atmospheric-marine salts rather than the water-rock interaction.

Since the frequent worldwide occurrence of this type of rock, it can be said that this kind of research is of widespread interest and these results can be transferred to other sites where granulite rocks occur.

Data Availability

The manuscript is a data self-contained article, whose results were obtained from the laboratory analysis, and the entire data is presented within the article. However, if any additional information is required, these are available from the corresponding author upon request to the e-mail apollaro@unical.it

Conflicts of Interest

The author declares that he has no conflicts of interest.

Acknowledgments

This research was carried out within the MIUR-ex 60% Project of Carmine Apollaro. The author is indebted to some anonymous reviewers and the Guest Editor Giovanni Mongelli for their useful discussions and suggestions on the manuscript. Special thanks go to Ilaria Fuoco for her useful suggestions on the manuscript.

References

[1] C. A. J. Appelo and D. Postma, *Geochemistry, Groundwaters and Pollution*, A.A. Balkema, Rotterdam, 1999.

[2] E. K. Berner and R. A. Berner, *Global Environment: Water, Air, and Geochemical Cycles*, Prentice Hall, Upper Saddle River, 1996.

[3] D. Hem, *Study and Interpretation of the Chemical Characteristics of Natural Water U.S. Geological Survey*, Water Supply Paper 2254, 1970.

[4] D. Langmuir, *Aqueous Environmental Geochemistry*, Prentice Hall, Upper Saddle River, 1997.

[5] C. Apollaro, L. Marini, and R. De Rosa, "Use of reaction path modeling to predict the chemistry of stream water and groundwater: a case study from the Fiume Grande valley (Calabria, Italy)," *Environmental Geology*, vol. 51, no. 7, pp. 1133–1145, 2007.

[6] C. Apollaro, L. Marini, R. de Rosa, P. Settembrino, F. Scarciglia, and G. Vecchio, "Geochemical features of rocks, stream sediments, and soils of the Fiume Grande Valley (Calabria, Italy)," *Environmental Geology*, vol. 52, no. 4, pp. 719–729, 2007.

[7] I. Guagliardi, C. Apollaro, F. Scarciglia, and R. De Rosa, "Influence of particle-size on geochemical distribution of stream sediments in the Lese river catchment, southern Italy," *Biotechnology, Agronomy, Society and Environment*, vol. 17, no. 1, pp. 43–55, 2013.

[8] I. Guagliardi, G. Buttafuoco, C. Apollaro, A. Bloise, R. De Rosa, and D. Cicchella, "Using gamma-ray spectrometry and geostatistics for assessing geochemical behaviour of radioactive elements in the Lese catchment (southern Italy)," *International Journal of Environmental Research*, vol. 7, pp. 645–658, 2013.

[9] F. Scarciglia, R. De Rosa, G. Vecchio, C. Apollaro, G. Robustelli, and F. Terrasi, "Volcanic soil formation in Calabria (southern Italy): the Cecita Lake geosol in the late Quaternary geomorphological evolution of the Sila uplands," *Journal of Volcanology and Geothermal Research*, vol. 177, no. 1, pp. 101–117, 2008.

[10] M. Accornero and L. Marini, "The double solid reactant method for modeling the release of trace elements from dissolving solid phases: I. Outline and limitations," *Environmental Geology*, vol. 55, no. 8, pp. 1627–1635, 2008.

[11] C. N. Alpers and D. K. Nordstrom, "Geochemical modeling of water-rock interactions in mining environments," in *The Environmental Geochemistry of Mineral Deposits, Chapter: 14*, G. S. Plumlee and M. J. Logsdon, Eds., pp. 289–324, Society for Economic Geologists, 1999.

[12] C. Apollaro, M. Accornero, L. Marini, D. Barca, and R. de Rosa, "The impact of dolomite and plagioclase weathering on the chemistry of shallow groundwaters circulating in a granodiorite-dominated catchment of the Sila Massif (Calabria, Southern Italy)," *Applied Geochemistry*, vol. 24, no. 5, pp. 957–979, 2009.

[13] C. Apollaro, L. Marini, T. Critelli et al., "Investigation of rock-to-water release and fate of major, minor, and trace elements in the metabasalt–serpentinite shallow aquifer of Mt. Reventino (CZ, Italy) by reaction path modelling," *Applied Geochemistry*, vol. 26, no. 9-10, pp. 1722–1740, 2011.

[14] J. Bruni, M. Canepa, G. Chiodini et al., "Irreversible water–rock mass transfer accompanying the generation of the neutral, Mg–HCO3 and high-pH, Ca–OH spring waters of the Genova province, Italy," *Applied Geochemistry*, vol. 17, no. 4, pp. 455–474, 2002.

[15] F. Cipolli, B. Gambardella, L. Marini, G. Ottonello, and M. Vetuschi Zuccolini, "Geochemistry of high-pH waters from serpentinites of the Gruppo di Voltri (Genova, Italy) and reaction path modeling of CO2 sequestration in serpentinite aquifers," *Applied Geochemistry*, vol. 19, no. 5, pp. 787–802, 2004.

[16] T. Critelli, G. Vespasiano, C. Apollaro, F. Muto, L. Marini, and R. De Rosa, "Hydrogeochemical study of an ophiolitic aquifer: a case study of Lago (Southern Italy, Calabria)," *Environment and Earth Science*, vol. 74, no. 1, pp. 533–543, 2015.

[17] H. C. Helgeson, "Evaluation of irreversible reactions in geochemical processes involving minerals and aqueous solutions: I. Thermodynamic relations," *Geochimica et Cosmochimica Acta*, vol. 32, no. 8, pp. 853–877, 1968.

[18] H. C. Helgeson, R. M. Garrels, and F. T. Mackenzie, "Evaluation of irreversible reactions in geochemical processes involving minerals and aqueous solutions: II. Applications," *Geochimica et Cosmochimica Acta*, vol. 33, no. 4, pp. 455–481, 1969.

[19] B. Merkel, B. Planer-Friedrich, and D. K. Nordstrom, *Groundwater Geochemistry: a Practical Guide to Modeling of Natural and Contaminated Aquatic Systems*, Springer Verlag, 2008.

[20] C. Zhu and G. M. Anderson, *Environmental Applications of Geochemical Modeling*, Cambridge University Press, UK, 2002.

[21] T. W. Wolery and R. L. Jarek, "Software user's manual," in *EQ3/6, Version 8.0. Sandia National Laboratories—U.S*, Department of Energy Report, 2003.

[22] M. L. Amodio, G. Bonardi, V. Colonna et al., "L'arco Calabro-Peloritano nell'orogene Appenninico Maghrebide," *Memorie della Societa Geologica Italiana*, vol. 17, pp. 1–60, 1976.

[23] E. Maccarrone, A. Paglionico, G. Piccarreta, and A. Rottura, "Granulite-amphibolite facies metasediments from the Serre (Calabria, Southern Italy): their protoliths and the processes controlling their chemistry," *Lithos*, vol. 16, no. 2, pp. 95–111, 1983.

[24] V. Schenk, "U-Pb and Rb-Sr radiometric dates and their correlation with metamorphic events in the granulite-facies basement of the serre, Southern Calabria (Italy)," *Contributions to Mineralogy and Petrology*, vol. 73, no. 1, pp. 23–38, 1980.

[25] R. Cirrincione, E. Fazio, P. Fiannacca, G. Ortolano, A. Pezzino, and R. Punturo, "The Calabria Peloritani Orogen, a composite terrane in Central Mediterranean; its overall architecture and geodynamic significance for a pre-Alpine scenario around the Tethyan basin," *Periodico di Mineralogia*, vol. 84, pp. 701–749, 2015.

[26] C. Tansi, F. Muto, S. Critelli, and G. Iovine, "Neogene-Quaternary strike-slip tectonics in the central Calabrian Arc (southern Italy)," *Journal of Geodynamics*, vol. 43, no. 3, pp. 393–414, 2007.

[27] F. Ietto, F. Perri, and F. Cella, "Geotechnical and landslide aspects in weathered granitoid rock masses (Serre Massif, southern Calabria, Italy)," *Catena*, vol. 145, pp. 301–315, 2016.

[28] D. Dietrich, S. Lorenzoni, P. Scandone, E. Zanettin-Lorenzoni, and M. Di Pierro, "Contribution to the knowledge of the tectonic units of Calabria; relationships between composition of K-white micas and metamorphic evolution," *Bollettino della Societa Geologica Italiana*, vol. 95, no. 1-2, pp. 193–217, 1976.

[29] V. Schenk, "Petrology of Felsic Granulites, Metapelites, Metabasics, Ultramafics, and Metacarbonates from southern Calabria (Italy): prograde metamorphism, uplift and cooling of a former lower crust," *Journal of Petrology*, vol. 25, no. 1, pp. 255–296, 1984.

[30] C. Apollaro, F. Perri, E. Le Pera, F Ilaria, and T. Critelli, *Chemical and Minero-Petrographical Changes on Granulite Rocks Affecting by Weathering Processes*, Front Earth Science, 2019.

[31] G. Rizzo, E. Piluso, and L. Morten, "Phlogopite-bearing ultramafic rocks from the Serre massif, Calabrian Peloritan Arc, southern Italy: an example of hybridization between hydrous siliceous melts and peridotites?," *Geologica Acta*, vol. 3, pp. 81–96, 2004.

[32] G. Rizzo, E. Piluso, and L. Morten, "Tonalitic to trondhjemitic dykes within metabasic lower-crust rocks, Serre Massif, Calabrian-Peloritan arc," *Bollettino Societa Geologica Italiana*, vol. 4, pp. 45–52, 2005.

[33] T. W. Wolery and C. Jove-Colon, *Qualification of Thermodynamic Data for Geochemical Modeling of Mineral-water Interactions in Dilute Systems*, Sandia National Laborato-ries Report, 2007, ANL-WIS-GS-000003 REV 01.

[34] L. Marini, *Geological Sequestration of Carbon Dioxide - Thermodynamics, Kinetics, and Reaction Path Modeling*, Developments in Geochemistry, 2007.

[35] H. C. Helgeson, J. M. Delany, H. W. Nesbitt, and D. K. Bird, "Summary and critique of the thermodynamic properties of rock-forming minerals," *American Journal of Science*, vol. 278, pp. 1–229, 1978.

[36] C. Apollaro, L. Marini, T. Critelli, and R. De Rosa, "The standard thermodynamic properties of vermiculites and prediction of their occurrence during water–rock interaction," *Applied Geochemistry*, vol. 35, pp. 264–278, 2013.

[37] C. Apollaro, L. Marini, T. Critelli et al., "Modeling of the impact of dolomite and biotite dissolution on vermiculite composition in a gneissic shallow aquifer of the Sila Massif (Calabria, Italy)," *Applied Geochemistry*, vol. 35, pp. 297–311, 2013.

[38] F. Perri, F. Scarciglia, C. Apollaro, and L. Marini, "Characterization of granitoid profiles in the Sila Massif (Calabria, southern Italy) and reconstruction of weathering processes by mineralogy, chemistry, and reaction path modeling," *Journal of Soils and Sediments*, vol. 15, no. 6, pp. 1351–1372, 2015.

[39] J. Majzlan, A. Navrotsky, and U. Schwertmann, "Thermodynamics of iron oxides: part III. Enthalpies of formation and stability of ferrihydrite (~$Fe(OH)_3$), schwertmannite (~$FeO(OH)_{3/4}(SO_4)_{1/8}$), and ε-$Fe_2O_3$," *Geochimica et Cosmochimica Acta*, vol. 68, no. 5, pp. 1049–1059, 2004.

[40] G. A. Brook, M. E. Folkoff, and E. O. Box, "A world model of soil carbon dioxide," *Earth Surface Processes and Landforms*, vol. 8, no. 1, pp. 79–88, 1983.

[41] B. W. Christenson and C. P. Wood, "Evolution of a vent-hosted hydrothermal system beneath Ruapehu Crater Lake, New Zealand," *Bulletin of Volcanology*, vol. 55, no. 8, pp. 547–565, 1993.

[42] L. Marini and G. Ottonello, Eds., *Atlante degli acquiferi della Liguria*, vol. 3, Le acque dei complessi ofiolitici, Pisa, 2003, bacini: Arrestra, Branega, Cassinelle, Cerusa, Erro, Gorzente, Leira, Lemme, Lerone, Orba, Piota, Polcevera, Rumaro, Sansobbia, Stura, Teiro, Varenna, Visone. Pacini Editore,.

[43] M. H. Reed, "Hydrothermal alteration and its relationships to ore fluids composition," in *Geochemistry of Hydrothermal Ore Deposits*, H. L. Barnes, Ed., pp. 303–365, Wiley, 1997.

[44] C. Apollaro, I. Fuoco, G. Brozzo, and R. De Rosa, "Release and fate of Cr (VI) in the ophiolitic aquifers of Italy: the role of Fe (III) as a potential oxidant of Cr (III) supported by reaction path modelling," *Science of the Total Environment*, vol. 660, pp. 1459–1471, 2019.